DR. 349

FE-2341-11
Dist. Category UC-90G

A HIGH MAGNETIC FIELD MHD GENERATOR PROGRAM

Quarterly Report
for the period
October to December, 1978

Stanford University
Stanford, California 94305

Date Published - January, 1979

Prepared for
THE UNITED STATES DEPARTMENT OF ENERGY
Under Contract No. EX 76-C-01-2341

A HIGH MAGNETIC FIELD MHD GENERATOR PROGRAM

Quarterly Report for the
Period October to December, 1978
Contract No. EX 76-C-01-2341

Prepared For
THE UNITED STATES DEPARTMENT OF ENERGY

Submitted by

Profs. R. H. Eustis, C. H. Kruger and M. Mitchner,
Adjunct Prof. S. A. Self, and Dr. J. K. Koester

January, 1979

High Temperature Gasdynamics Laboratory
Department of Mechanical Engineering
Stanford University

Foreword

Much of the work on this program is carried out by student Research Assistants and High Temperature Gasdynamics Laboratroy staff members in addition to the Principal Investigators. The additional persons involved in a major way with the work reported here are

Dr. Takashi Nakamura
Mr. John P. Barton
Mr. Bradford Bennett
Mr. Kent James
Mr. Marion Jenkins
Mr. Ralph Kowalik

TABLE OF CONTENTS

List of Figures

ABSTRACT

The modifications to the High Temperature Gasdynamics Laboratory were completed so that space is available for the 7 tesla superconducting magnet to be furnished by the Department of Energy. The continued analysis of the fluctuations in the MHD channel showed standing acoustic waves and the presence of non-uniformities convected with the flow. Further development of the laser fluorescence technique to measure temperature and seed concentration with 3-dimensional spatial resolution for time varying flows was undertaken with good success. Preparations continued for three experiments to be run next quarter--an electrode boundary layer experiment to investigate Joule heating effects, a thermal check-out of the 6 tesla disk generator system and a thermal check-out of the 6 tesla linear channel

1.0 OBJECTIVE AND SCOPE OF WORK

The objective of this program is to investigate the high magnetic field effects in MHD channels which will influence the design of large scale generators. The work includes the study at high fields of 1) plasma nonuniformities and instabilities and 2) boundary layer and Hall field phenomena. In addition a third activity is centered on the existing Stanford 6 tesla magnet where small scale linear and disk channels are investigated.

2.0 SUMMARY OF PROGRESS, October to December, 1978.

The tasks of the contract statement of work have been grouped into three Work Areas as shown in Table 1, Milestones for MHD Research at High Magnetic Fields. The Work Areas which are keyed to the program objectives are

I Plasma Nonuniformities and Instabilities

II Boundary Layer and Hall Field Phenomena

III Six Tesla Magnet Investigations

The modifications of the High Temperature Gasdynamics Laboratory test facilities were completed during the present quarter and space is now available for the 7 tesla superconducting magnet to be furnished by the Department of Energy under the conditions of the contract.

In the investigation of possible instabilities in MHD generators, further analysis of the data obtained during the experiments of last quarter was made. The present analysis utilized spectral density, autocorrelation, cross correlation, coherency, relative phase, and probability distribution functions. For the non-interaction experiments for which j and B were not simultaneously present, the behavior of the channel was acoustic in nature with standing pressure waves present. By making measurements for the open circuit generator case and with applied voltages ($B = 0$) it appears that nonuniformities in conductivity can be reasonably postulated. These regions of high and low conductivity are convected with the gas and will influence the performance of the generator.

The laser fluorescence diagnostic which is being developed to make a direct measurement of possible non-uniformities was investigated on the bench under time-varying conditions. A comparison was made with two other diagnostics simultaneously and the laser fluorescence technique appeared to work well. A theoretical analysis of the effect of magnetic field on spectral

line-splitting was made with the result that the field will decrease the sensitivity of the measurement. More powerful lasers would improve this possible problem.

Preparations continued for an experiment to measure Joule heating phenomena in electrode boundary layers. Diagnostic development and electronics construction is making good progress. The electrode boundary layer computer program is being improved and will be useful for future studies as well as for comparison between theory and the results of the current experiment.

The construction of the 6 tesla disk and linear channels progressed well and the test facility is being readied for thermal checkouts of both channels next quarter.

The status of the work is summarized in the Program Milestone Chart, Figure 1.

Table 1

Milestones for MHD Research at High Magnetic Fields

WORK AREA I - Plasma Nonuniformities and Instabilities

Task 1 Plasma Nonuniformity Study

1.1	Initiate development of pressure fluctuation diagnostics
1.2	Test of diagnostics in cold channel
1.3	Test of diagnostics of M-2 channel

Task 2 Development of Temperature Fluctuation Diagnostics

2.1	Initiate bench development of rapid line reversal method
2.2	Apply rapid line reversal method to open burner
2.3	Apply rapid line reversal method to M-8 channel
2.4	Bench development of laser system for spatial resolution
2.5	Apply laser system to open burner
2.6	Apply laser system to M-8 channel

Task 3 Instabilities

3.1	Tests of fluctuation in cold channel (see 1.2)
3.2	Initiate test with normal operating conditions in M-2
3.3	Initiate test with introduced disturbances in M-2

WORK AREA II - Boundary Layer and Hall Field Phenomena

Task 4 Boundary Layer Study

4.1a	Develop LDV techniques
4.1b	Develop line intensity techniques
4.1c	Develop line reversal techniques
4.1	Initiate development of technique for remote channel operation
4.4	Extend theory to large MHD channels

Task 5 Turbulence Damping Study

Task 6 Hall Field Limitation Study

6.1	Initiate electrode development for Super M-8 channel

Task 7 Electrode Configuration Study

7.2	Preliminary test of electrode in M-2 channel

Task 8 Current Concentration

8.1	Initiate development of segmented electrode
8.2	Test segmented electrode in M-2 channel

WORK AREA III - Six Tesla Magnet Investigations

Task 9 Disk Generator Program

9.1a Complete construction of disk generator
9.1b Complete construction of disk generator exhaust system
9.2 Thermal checkout of disk system
9.3 Test in 6 tesla magnet

Task 10 Linear Six Tesla Channel

10.1 Complete design of linear channel for 6 tesla magnet
10.2 Complete construction of linear channel
10.3 Thermal test outside of magnet
10.4 Experiment in 6 tesla magnet with clean fuel
10.5 Test in 6 tesla magnet with coal combustion

HIGH MAGNETIC FIELD
MHD GENERATOR PROGRAM
Technical Work Areas

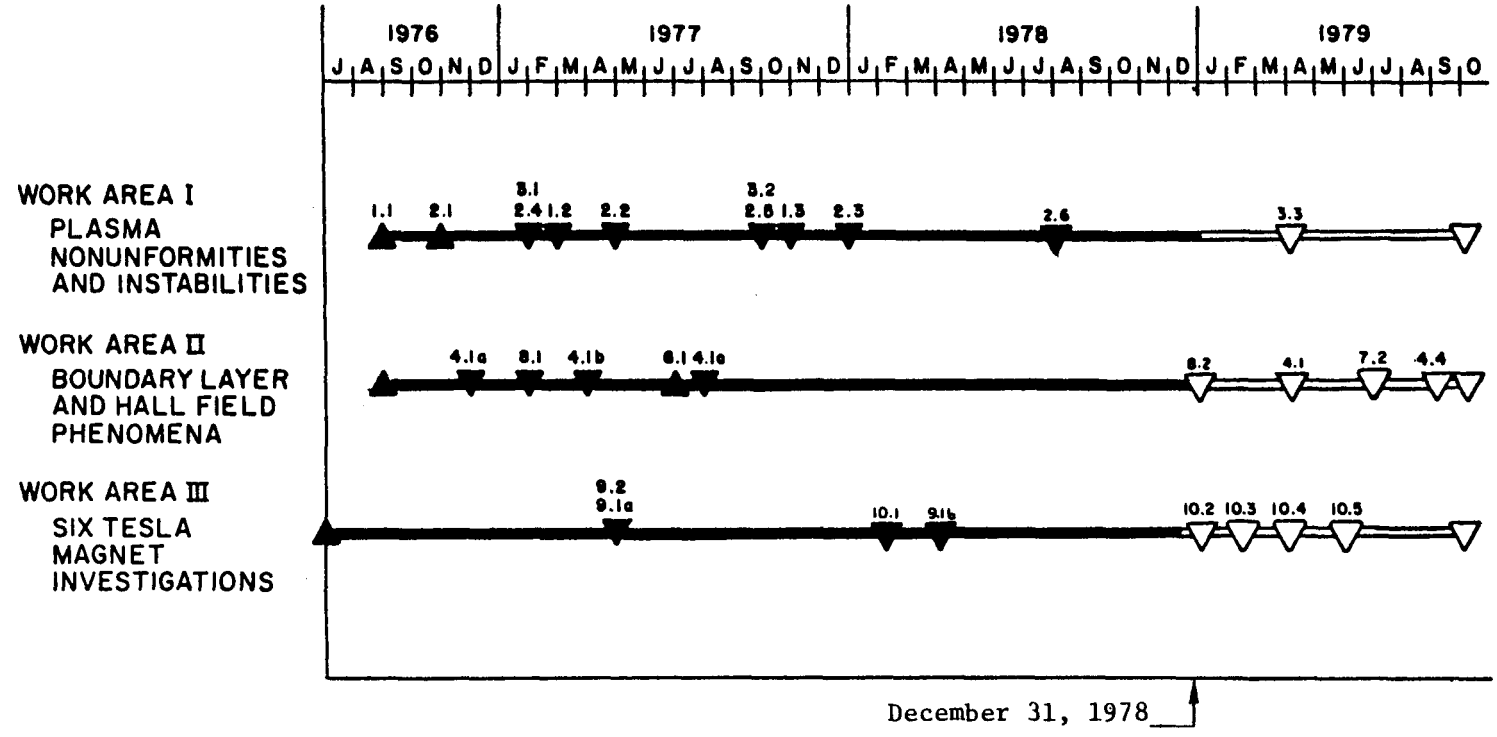

Figure 1. Program Milestone Chart.

3.0 DESCRIPTION OF TECHNICAL PROGRESS

3.1 Work Area I - Plasma Nonuniformities and Instabilities

3.1.1 Plasma Instability Investigation.

Analysis of the data obtained from the series of magneto-acoustic experiments performed in July 1978 continued. These experiments involved the measurement and study of inherent fluctuations in current, electric field, and pressure within the Stanford M-2 generator facility as a function of system operating parameters. A description of the experimental apparatus was presented in the July 1, 1977 to June 30, 1978 Annual Report. A preliminary examination of the root-mean-square amplitudes of the fluctuating quantities was given in the July - September 1978 quarterly report. Subsequently, the measurements have been analyzed using other statistical techniques. The spectral density, autocorrelation, cross correlation, coherency, relative phase, and probability distribution functions have been utilized to determine essential features of the data. Further insight has been gained from these analyses.

One goal of the experiments was to establish the structure of the inherent disturbances within the combustion plasma so that the effect upon MHD generator performance could be better understood. For this purpose, experimental measurements were taken not only with the generator operating in the normal power generation mode, but measurements were also made for the background, noninteraction case of no current or applied magnetic field. Other conditions included runs with applied magnetic field only (generator open circuit) and runs with externally applied electric field only (no applied magnetic field). Analyses of these cases provide information concerning the nature of the background nonuniformities. In the discussion that follows typical reduced data are presented that display important features of the observed phenomena. For reference, Figure 2 shows the relative orientation of the measurements that were made during the experiments.

Noninteraction Measurements

Background pressure fluctuations in the generator channel were found to be predominantly acoustic in nature and to exhibit the presence of normal standing waves. Pressure fluctuation measurements taken at one axial location correlate strongly with those taken at another axial location. The two measurements are in phase to a certain frequency and then go out of phase. These observations are demonstrated by the coherency function and relative phase function between upstream and downstream pressure, for one experimental case, given in Figure 3. This type of behavior is characteristic of acoustic standing waves. Hydrodynamic pressure oscillations would be expected

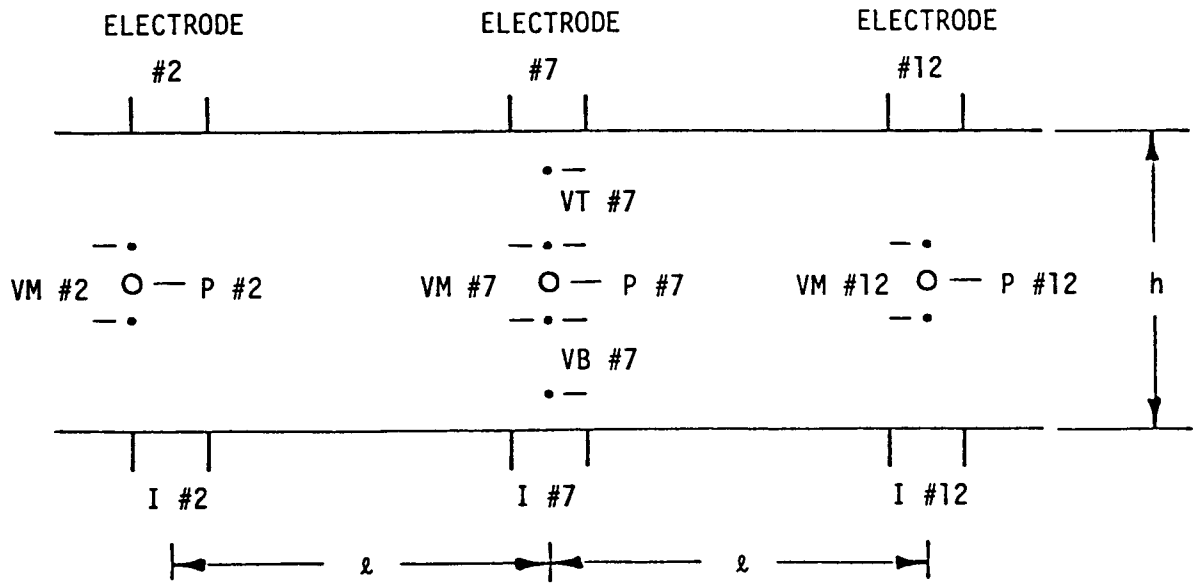

Figure 2. Position of fluctuation measurements taken in July 1978 magnetoacoustic experiments. Inherent fluctuations in current (I), transverse electric field (V), and pressure (P) were measured at three electrode positions: upstream (electrode #2), middle (electrode #7), and downstream (electrode #12). Generator channel dimensions: channel height h = 10 cm, channel width w = 3 cm, distance between measurement locations ℓ = 19 cm.

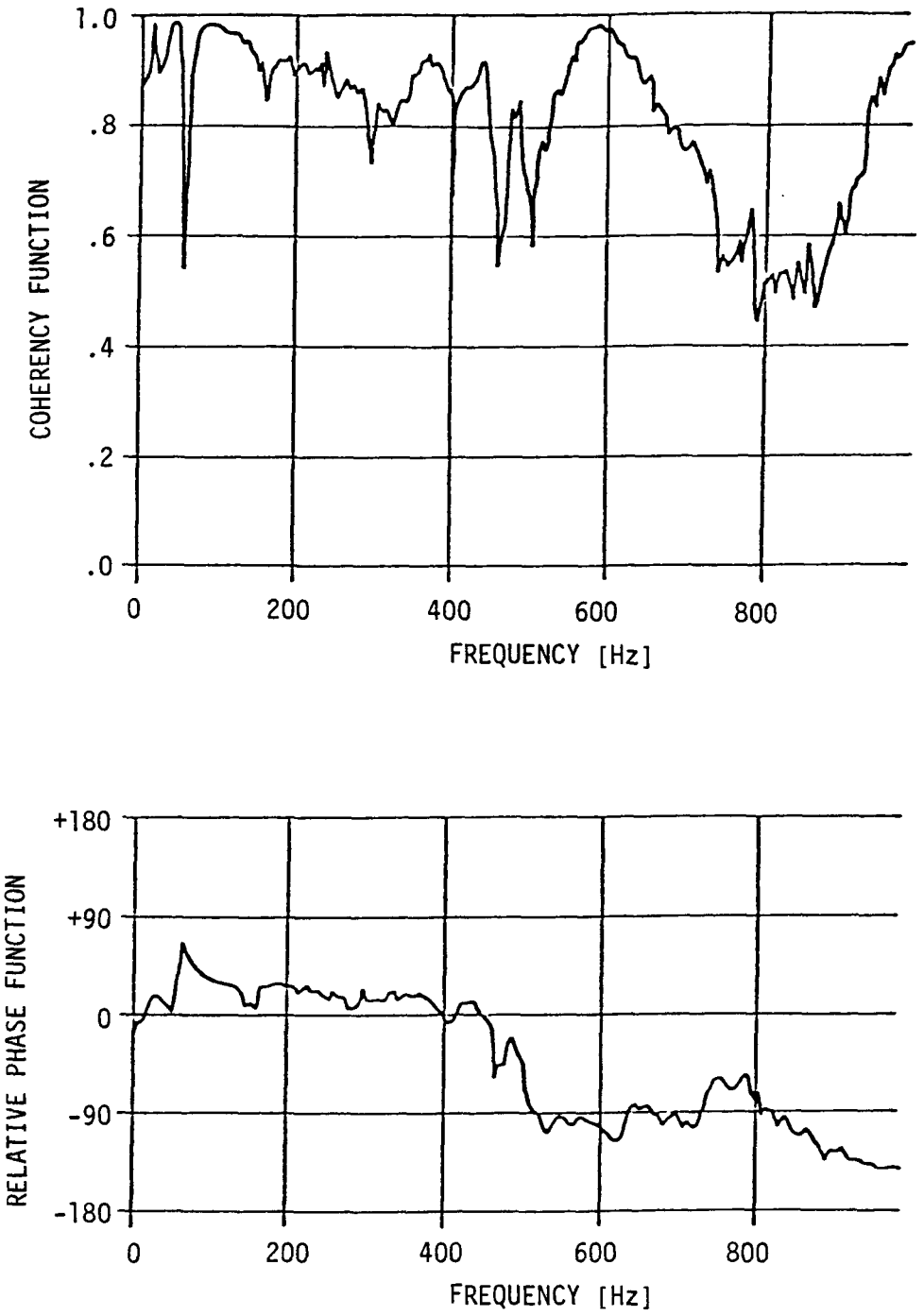

Figure 3. The coherency function and relative phase function for upstream pressure versus downstream pressure. Generator operating at open circuit with no applied magnetic field. System conditions: $\dot{m}$ = .15 (lbm/s), N_2/O_2 = .0, B = 0(T).

to correlate poorly from one axial location to another and, if correlated, to correlate in a convected manner.

Open Circuit Generator Measurements

The velocity oscillations associated with the existing acoustic waves produced measurable induced electric field fluctuations. With the generator operating at open circuit the induced voltage provides an indication of velocity. The fluctuations in voltage with applied magnetic field, for the case of no current, correlated strongly and in phase in the transverse direction (measured at location #7) demonstrating a one dimensional, axial disturbance in velocity. Oscillations in induced voltage also correlated well in the flow direction showing a similar in-phase, out-of-phase behavior as that exhibited by the background pressure measurements.

Velocity amplitudes calculated from the measured induced voltages compare reasonably with the velocity amplitudes expected to be associated with the measured level of acoustic pressure. Frequency spectra of the induced voltage fluctuations measured across the electrodes during generator open circuit operation showed the same frequency character as the background pressure (see Figure 4). Characteristic frequencies are exhibited. The higher frequency peaks, occurring for this set of flow parameters at approximately 600 Hz and 1000 Hz, have been attributed to the natural acoustic modes of the generator channel. The two low frequency peaks, for this case at approximately 30 Hz and 70 Hz, have been attributed to natural resonances of the MHD system including the combustor and exhaust sections. The voltage and pressure fluctuations at the same location are strongly correlated. The coherence function and relative phase function between pressure and voltage for a given open circuit condition are shown in Figure 5. The voltage is alternately in and out of phase with the pressure in a manner similar to the velocity in normal acoustic standing waves. Study of the relative phase functions for this case can provide information concerning the acoustics of the system.

No Magnetic Field, Externally Powered Generator Measurements

The generator was also run in the applied electric field configuration in which there was no magnetic field and thus no induced voltages. For this case generator voltages and currents respond primarily to the plasma conductivity. The measured fluctuations in current and voltage were found to be much larger than what one would expect for the conductivity fluctuations that would be associated with the acoustic standing waves. In addition, the frequency spectra of the current and voltage fluctuations for this case, shown typically in Figure 6, exhibit a smooth falloff character in contrast with the frequency spectra of the acoustical measurements which had

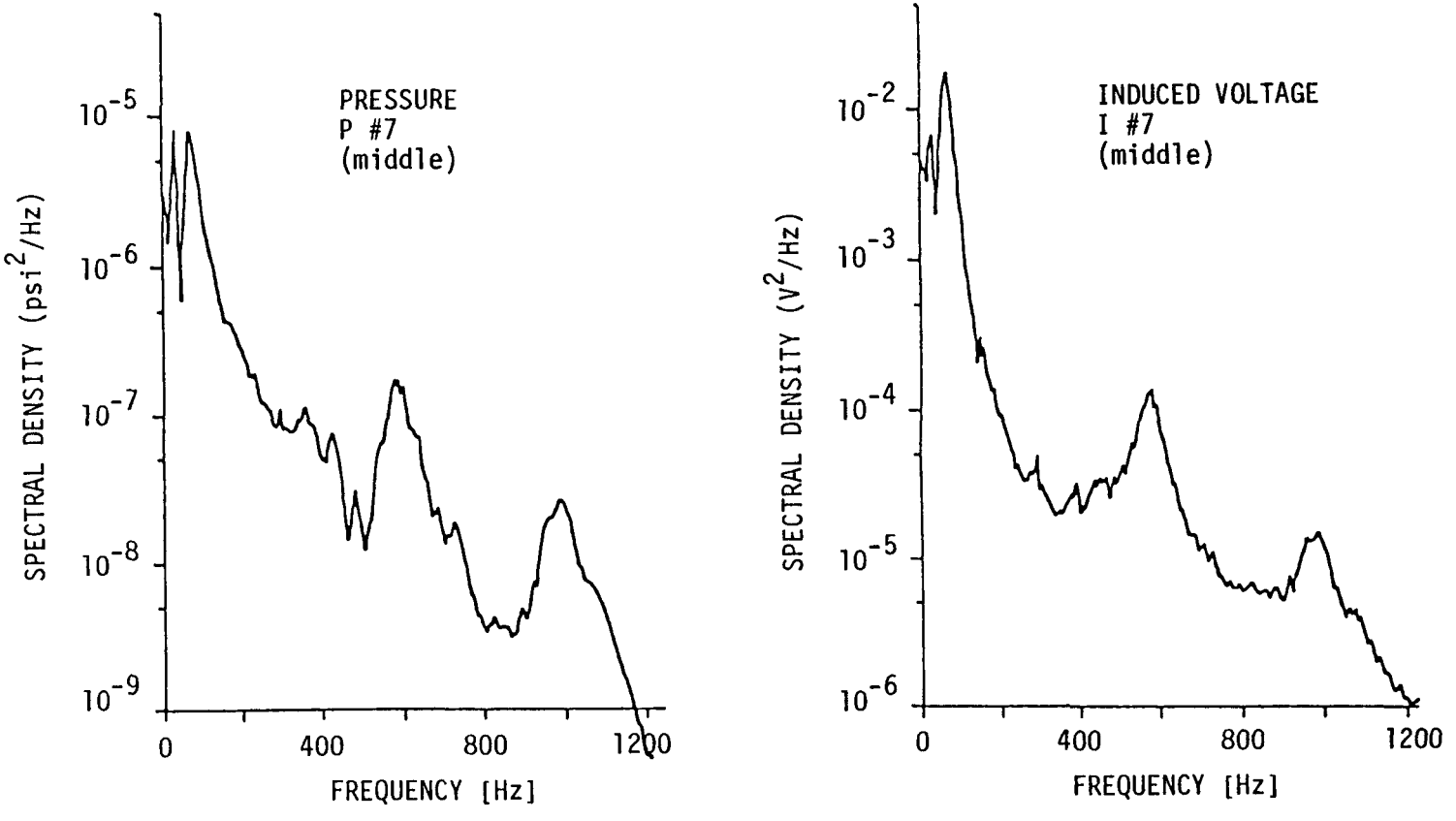

Figure 4. Frequency spectra of measured pressure and electrode voltage at middle channel location. Generator operating at open circuit with applied magnetic field. System conditions: $\dot{m}$ = .2 (lbm/s), N_2/O_2 = .0, B = 2.4 (T).

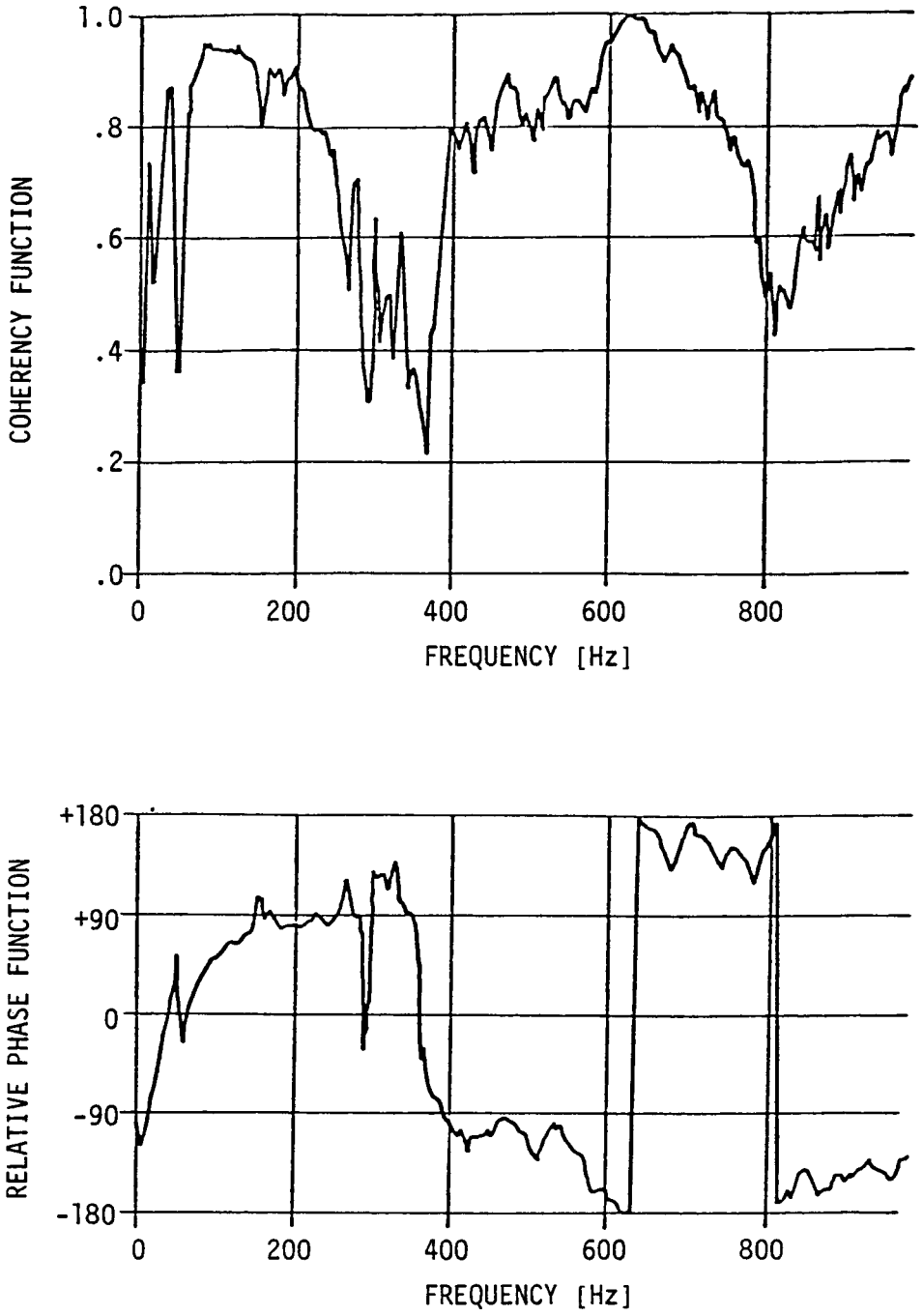

Figure 5. The coherency function and the relative phase function for pressure versus electrode voltage at middle channel location. Generator operating at open circuit with applied magnetic field. System conditions: $\dot{m}$ = .2 (lbm/s), N_2/O_2 = .0, B = 2.4 (T).

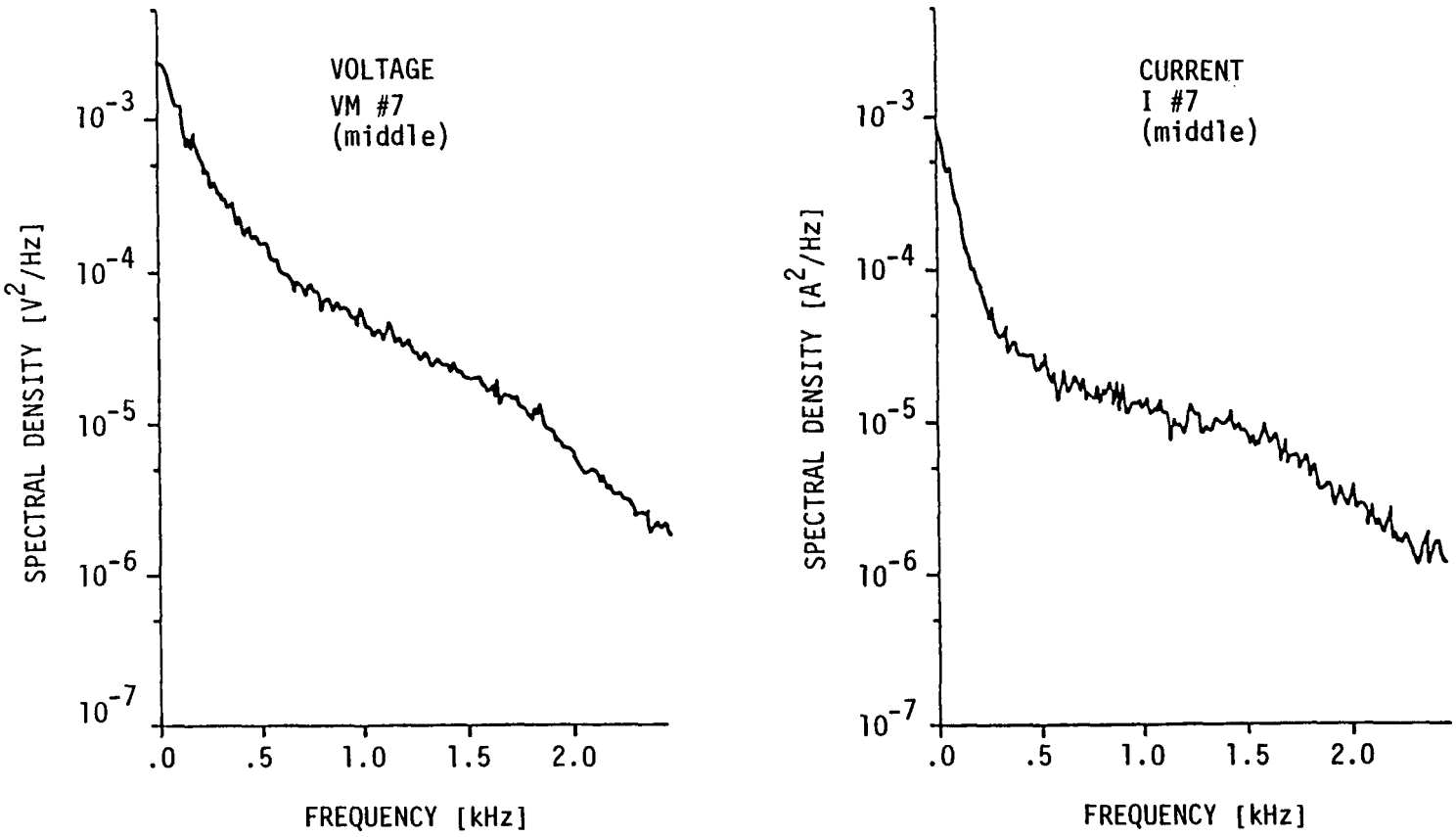

Figure 6. Frequency spectra of inner pin transverse voltage and electrode current at middle channel location. Generator operating with applied electric field and no applied magnetic field. System conditions: $\dot{m}$ = .2 (lbm/s), N_2/O_2 = .0, B = 0.(T), J = .7 (A/cm^2).

characteristic peaks (compare with Figure 4). Fluctuations in pressure, which have been demonstrated to be acoustic, correlate poorly with both current and voltage fluctuations for this condition demonstrating that the origins of these two types of disturbance are independent.

Electrical measurements for the applied electric field case show a strong correlation in the axial direction with a maximum correlation at a delay time corresponding with the flow time between the two points of measurement. The conductivity inhomogeneities are thus convective in nature. A sample cross correlation is given in Figure 7. The average flow velocity between two points can be computed from the formula $V_{ave} = \ell/\Delta\tau$ where ℓ is the distance between the two points of measurement and $\Delta\tau$ is the delay time for correlation read from the cross-correlogram. Velocities computed in this manner compare well with mean flow velocities derived independently. The coherency and relative phase function for the same data as presented in Figure 7 are shown in Figure 8. A high coherency is demonstrated at low frequency with the decrease in coherency at higher frequencies perhaps due to a breakup in fine structure of the inhomogeneities as they flow through the channel. The ramp like form of the relative phase function shows all frequencies are convected at the same velocity. The relative phase of convected phenomena is quite different from that demonstrated by standing wave phenomena (compare Figure 8 with Figure 3).

Though the voltage fluctuations correlated well in the axial direction, there was poor correlation in the transverse direction. Likewise, the current fluctuations, which represent an integrated effect of the conductivity non-uniformities, correlate poorly with the voltage fluctuations taken in the same region. The conductivity disturbances are thus pictured as three dimensional and convected as opposed to the acoustic standing waves which are axial and stationary. A representation of the disturbances within the background combustion plasma of the Stanford M-2 facility is schematically shown in Figure 9.

Short Circuit Generator Measurements

We have previously reported that at large interaction pressure fluctuation levels increased by a factor of up to four. Based on the inhomogeneity model inferred from the aforementioned measurements, this behavior may, in part, be related to fluctuations in the current-magnetic field interaction force that result from fluctuations in current caused by inhomogeneities in conductivity. The effect of these background non-uniformities on MHD generator performance are being studied both theoretically and experimentally. Further results and conclusions will be given in later reports.

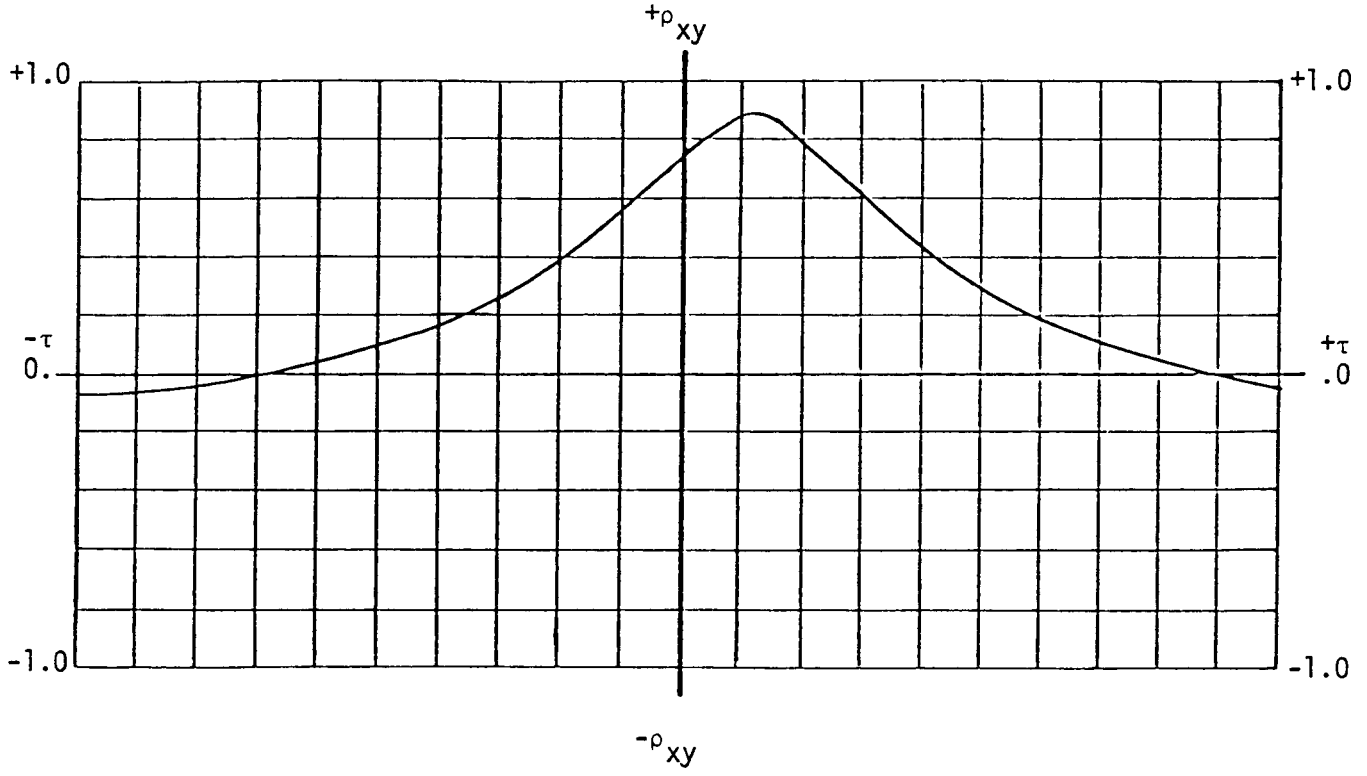

Figure 7. Cross correlation coefficient for upstream electrode current versus middle electrode current. Generator operating with applied electric field and no applied magnetic field. System conditions: $\dot{m}$ = .3(lbm/s), N_2/O_2 = .25, B = 0(T), J = .8(A/cm). Scale: .5 ms/div.

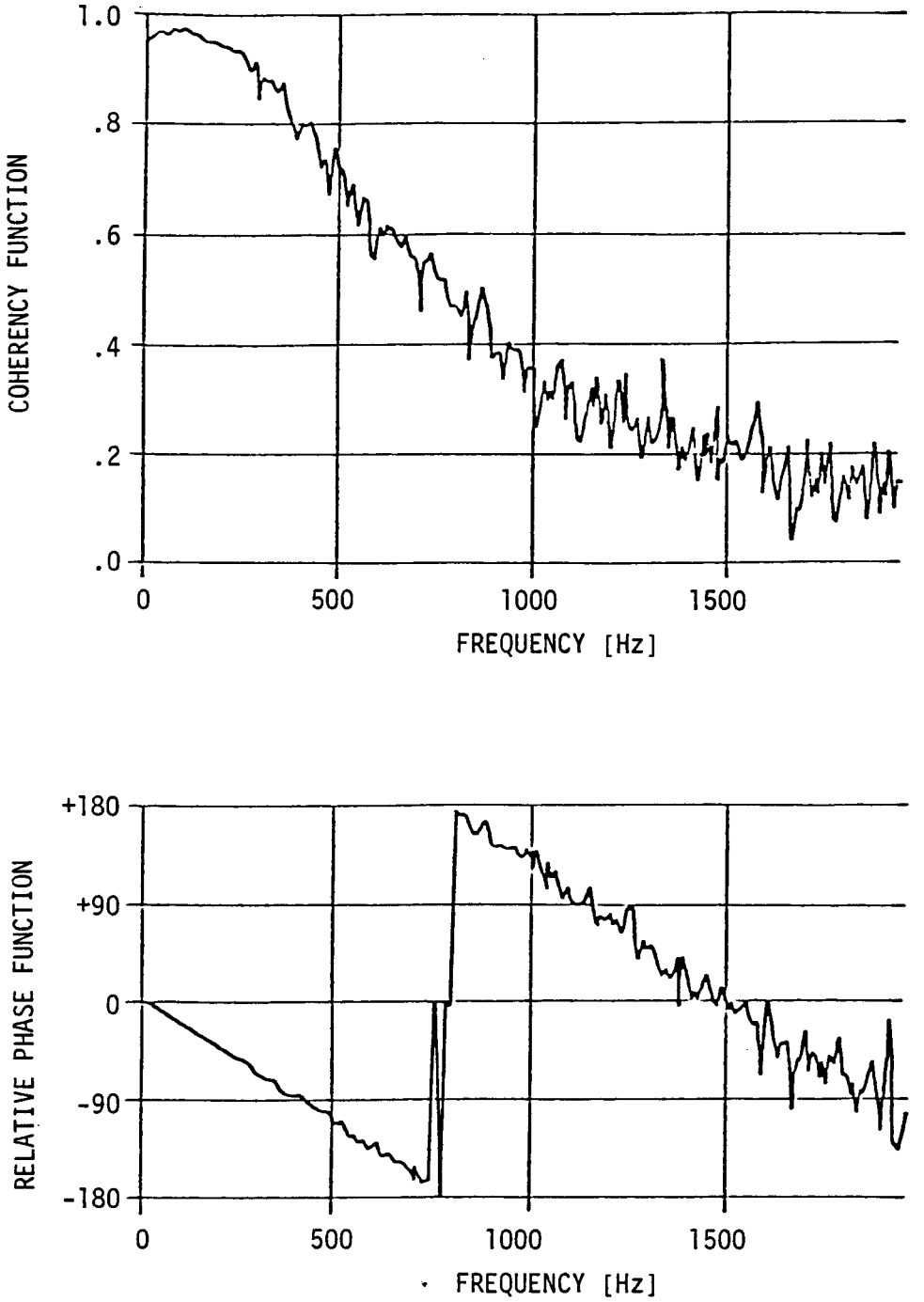

Figure 8. The coherency function and relative phase function for upstream electrode current versus middle electrode current. Generator operating with applied electric field and no applied magnetic field. System conditions: $\dot{m}$ = .3(lbm/s), N_2/O_2 = .25, B = 0.(T), J = .8(A/cm^2).

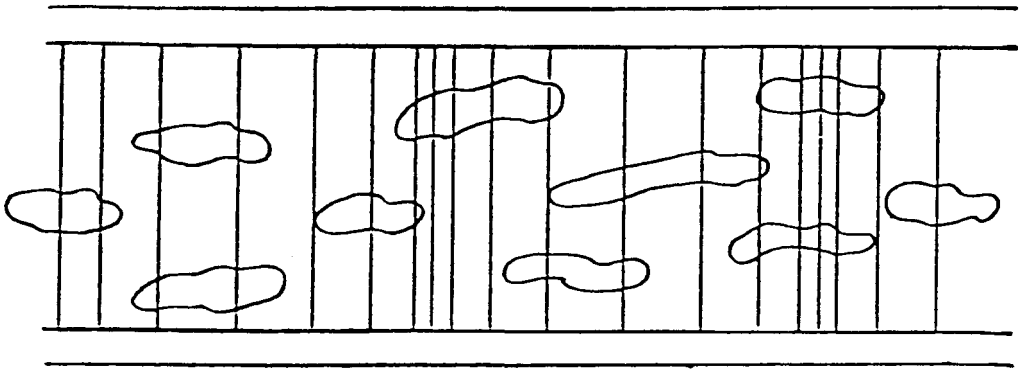

Figure 9. Representation of background inhomogeneities in the Stanford M-2 MHD facility channel. The disturbances consist of a combination of one dimensional, axial acoustic standing waves and three dimensional, convected conductivity inhomogeneities.

3.1.2 Plasma Nonuniformity Studies.

Construction in our laboratory has delayed the full-scale check-out of the laser-induced fluorescence diagnostic. These experiments are currently scheduled for January, 1979. Work has continued on two other aspects of diagnostic, namely, bench-top demonstrations of transient fluorescence measurements and theoretical calculations of the effects of magnetic fields on fluorescence measurements.

The transient fluorescence measurements were made with the Perkin-Elmer slot burner and fluctuation device which were used in the development of fluctuating line-reversal measurements [1]. Large 60 Hz fluctuations were introduced into the sodium seeded flame and monitored with three separate measurements. These included fluorescence measurements at 5688 Å (laser excitation @ 5682 Å), emission measurements at 5688 Å and emission measurements in the wing of the 5890 Å line. The 5688 Å measurements were made through a custom-made narrowband optical filter; the 5890 Å measurements were made with a monochromator. All of the measurements had a common line-of-sight perpendicular to the burner slot.

Examples of the measurements are shown on oscilloscope photographs in Figures 10 and 11. Figure 10 shows the three signals with the fluctuation device off. The dc levels have been adjusted to have approximately the same displacement on the oscilloscope. Figure 11 shows the same adjusted signals with the fluctuation device operating. In both figures the noisier trace corresponds to the fluorescence signal; the smoother traces are the emission signals.

Quantitative interpretation of these measurements is difficult since the exact nature of the introduced fluctuations is unknown, especially in the small fluorescing volume. The similarity of the three signals suggest that the fluctuations are predominantly in seed number density. Temperature fluctuations would have given the 5688 Å emission signal significantly larger fluctuation levels when compared with the other two signals. Path length fluctuations would have emphasized the two emission signals and not the local fluorescence signal. There is also a possibility of a combination of compensating fluctuations which may have produced the similar signals. Nevertheless, the important result of the experiments is that one could observe fluctuating fluorescence signals with the transient fluorescence configuation, which was the objective of these experiments.

The ultimate limitation of transient measurements will be the shot noise associated with the radiation measurements.

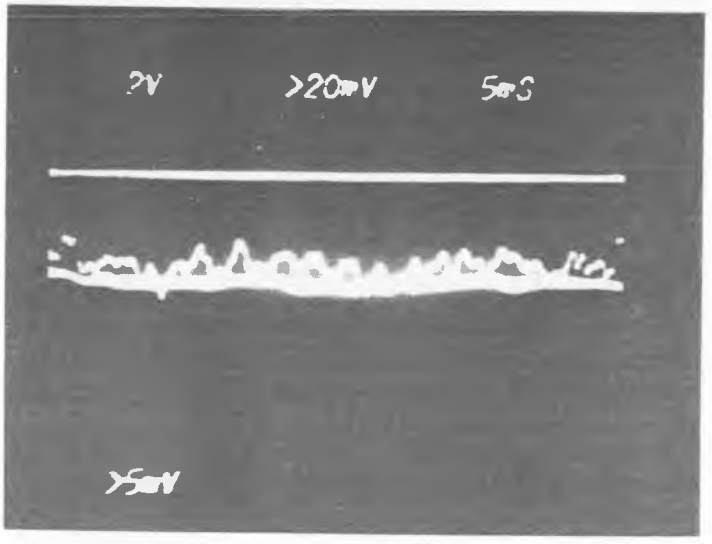

Figure 10. Flame signals with fluctuation device off.

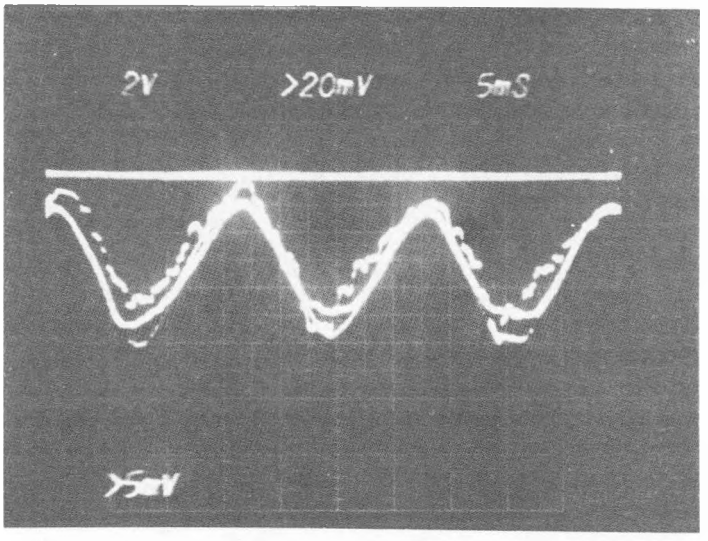

Figure 11. Flame signals with fluctuation device on.

The noise will come from two sources. Both the fluorescence signal and the background emission signal from the line-of-sight of the fluorescence measurement have shot noise contributions in the bandwidth of the lock-in amplifier. The background signal in an MHD channel is likely to be several hundred times larger than the fluorescence signal. Consequently, signal levels must be large enough such that the small percentage shot noise contributions of the relatively large background signal are still small when compared to fluctuations in the fluorescence signal. Shot noise contributions from the fluorescence signal will probably be negligible. Extrapolations of signal level measurements in the Perkin-Elmer burner suggest that 10% rms conductivity fluctuations with a bandwidth of 500 to 1000 Hz will be measurable in the Stanford M-2 channels. Uncertainties in seed concentration levels in the slot burner preclude more definite predictions. The minimum $\Delta\sigma/\sigma$ that can be observed for a given bandwidth should be clarified by the results of the January experiments.

Whatever bandwidth is obtainable in an MHD channel, it will be reduced in the presence of magnetic fields. The reduction is a net result of the splitting of the sodium 3p-4d spectral lines by the magnetic fields. Figure 12 shows the relative strengths and spacings of the 3p-4d lines in a magnetic field of 2 T. The spacings of 0.1 Å are approximately the same as the laser linewidth. Thus, in fields greater than or equal to 2 T only one of the split lines will be able to be excited with the laser. To first order, one could increase the seed concentration so that an equal number of atoms would be excited to the 4d sublevels. Then assuming that the fluorescence yield would be the same as in the unsplit case, an equally large fluorescence signal could be obtained. However, the increase in the seed concentration would increase the background signal and its shot noise contribution. When the excitation scheme of Figure 12 is used, the net result for a constant signal-to-noise ratio is a reduction of the bandwidth by a factor of 6.67. This theoretical result can be considered a minimum reduction which is inherent in the scheme. Limited optical access, photomultiplier shielding considerations, and the optical filter's bandshape may cause further reductions in both signal levels which would also decrease the bandwidth. Experiments to quantify the capabilities and limitations of the diagnostic in magnetic fields are planned for March-April, 1979. These experiments will be performed in the Stanford M-2 generator with a 5-watt argon-ion laser pumping the dye laser. More powerful lasers would improve the bandwidth capabilities of the diagnostic.

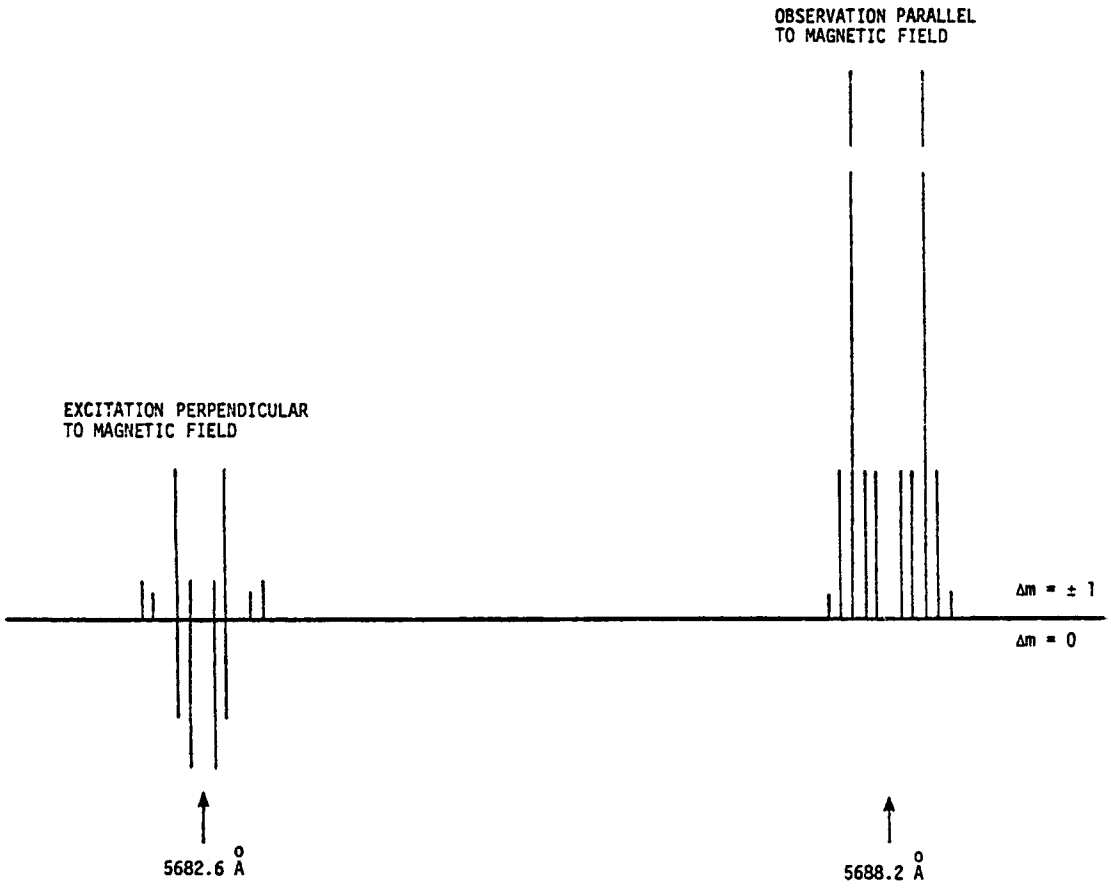

Figure 12. 4d-3p transitions of sodium in 2 T magnetic field.

3.2 Work Area II - Boundary Layer and Hall Field

3.2.1 Electrode Wall Profiles.

Preparation continued for an experiment to measure Joule heating phenomena in electrode wall boundary layers. A sidecover mirror mount with mirror purge and a pneumatically operated shield was developed to protect the mirrors that will be mounted on the sidecover as part of the spectroscopic system. New magnet spacers were designed to allow up to 5.75 inches of additional distance between the magnet pole caps, as the optical access in the upcoming experiment is accomplished by opening up the magnet to allow an image of the boundary layer to pass between the channel sidecover and the magnet polepieces. Although some difficulties are being experienced in assembling segmented electrodes for the Hall field breakdown portion of the experiment, progress is being made in overcoming the problems, and the assembly of the segmented electrodes is progressing.

Construction and testing of the two-dimensional temperature diagnostic continued. A linear fiber optic array was constructed by mounting 12 small fiber optics bundles in an aluminum holder. The fiber optic array was mounted in a box attached to the exit slit of the monochromator. A receiver for the fiber optics signals was constructed using 12 EG&G PV-100A photodiode detectors. A prototype amplifier was constructed for the photodiodes. This amplifier must be capable of detecting a signal of 10 picoamperes with a frequency response of 1000 Hz. Testing of the two-dimensional temperature measurement system revealed weaknesses in the photodiode amplifier design. The amplifier experienced stability problems due to the high gains involved, and in addition had unacceptable low-frequency noise and drift. The amplifier was redesigned using higher quality operational amplifiers (Analog Devices 515 K and 510 K), and the layout of components was changed to reduce unwanted feedback. A prototype of the new design seems to perform satisfactorily. Construction of 12 channels of photodiode amplifiers using the new design is now proceeding.

In addition to the preparations for the experiment, computer program development was done for data reduction and analysis. An existing electrode wall boundary layer computer program is being upgraded and documented with the intention of improving its capabilities. Recent additions to the program have included: 1) capabilities for handling two-dimensional current fields, 2) a core solver with options for area, velocity, density, pressure, or enthalpy specified in the marching procedure, 3) improved control and output facilities to allow easy simulation of experimental runs and output of experimentally measured quantities, 4) calculations of integral parameters, and performance parameters, to allow the program

to be used as a performance predictor. Present plans call for developing this program into a standardized boundary layer computer solver, to be used for evaluating a variety of present and future experiments, including MHD turbulent damping, Hall field breakdown, and electrode wall current transport effects.

3.3 Work Area III - Six Tesla Magnet Investigation

3.3.1 Disk Generator Program.

Fabrication of the new disk generator test section was completed. The entire generator flow system--combustor, plenum chamber, generator test section, exhaust manifold and exhaust duct--is currently being assembled for the thermal test. Progress was made in investigation of spatial and temporal stability of the current discharge in the r-θ plane of the generator. Performance prediction studies completed to date show that the radial inflow disk generator operating in the subsonic regime is satisfactory for base-load power and that the performance of such a disk generator is comparable to that of the diagonal generator.

Disk Generator Test Facility

Fabrication of the disk generator test section was completed. The upstream insulator plate and the downstream insulator plate without electrodes are shown in Figure 13. The surface of the upstream insulator plate is contoured for a constant Mach number flow. The surface of the downstream insulator plate is flat so as to accommodate electrodes of simple configurations. Each insulator element is directly soft-soldered to the water-cooled copper base plate. The size of the insulator elements is set to satisfy the empirical thermal stress criteria discussed in a previous contract report [2].

The generator test section and the exhaust manifold are being assembled around the mock-up of the superconducting magnet and the entire generator flow system--combustor, plenum chamber, generator test section, exhaust manifold and exhaust duct--will be tested with seeded combustion gas prior to the experiment with the superconducting magnet.

Performance Prediction Study

The performance characteristics of disk MHD generators was analyzed for the combustion products of a western coal at typical base-load conditions. Three disk generator configurations--radial outflow, radial inflow and radial inflow-outflow--were considered for both impulse and reaction modes of

a)

b)

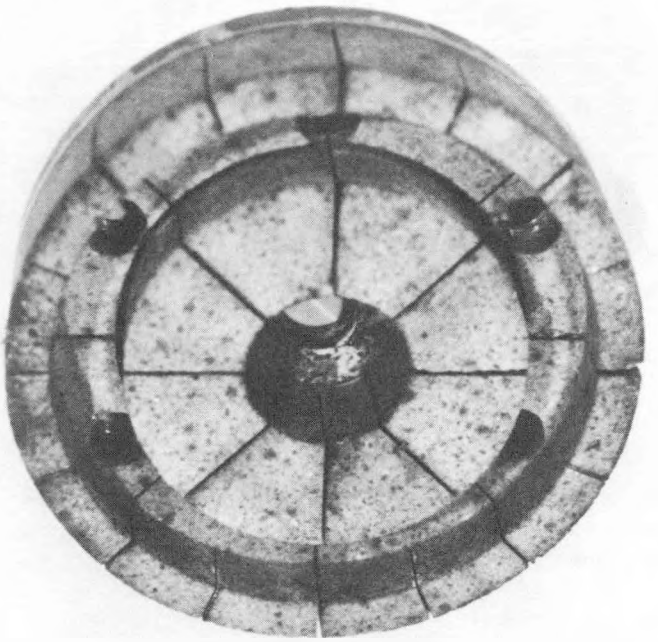

Figure 13. The upstream insulator plate (a) and the downstream insulator plate (b) without electrodes.

operation. It was shown that, in terms of enthalpy extraction, generator isentropic efficiency, electric fields to be sustained along the generator channel and simplicity of the generator channel geometry, the reaction mode radial inflow configuration is preferable for the base-load disk generator. The radial inflow-outflow configuration, which is a combination of the inflow and the outflow geometries, could attain higher performance than the radial inflow configuration with substantially reduced generator size. Comparison of disk generators with linear generators show that the performance of the disk generator is comparable to that of the diagonal generator, while the magnet cost for the disk generator is expected to be less than that for linear generators. More detailed information is given in the paper "Performance of Disk Generators for Open-cycle MHD Power Generation" which has been submitted to the 18th Symposium on Engineering Aspects of MHD to be held June 18-20,1979.

3.3.2 Linear Generator Program.

The construction of the peg wall channel described in earlier Quarterly Reports has progressed with completion of the fabrication of the walls and some pegs. Brazing techniques for the lanthanum-chromite electrodes are being further developed based on earlier successful attachment of samples. A hot test is scheduled for next quarter.

Detailed consideration has been given to the experimental program for the six tesla linear channel. It is planned to investigate the following phenomena at magnetic fields up to 6 tesla:

1. Effective conductivity
2. Effective Hall parameter
3. Effect of β and j on electrode voltage drops
4. Current concentration on electrodes
5. Boundary layer shear stress
6. Time dependent fluctuations

Both the effective conductivity and effective Hall parameter can be found if current and field magnitudes and directions are known in the generator channel. The generator is constructed with segmented electrodes with a pitch of 0.5 cm. By connecting the electrodes together in a continuous configuration and measuring the current to each segment, the current angle (and magnitude) can be ascertained. Probes will be used to measure the electric fields E_x and E_y in the core.

Electrode voltage drops are frequently measured by extrapolating voltage probe measurements in the core to the electrode wall and comparing the actual electrode voltage with the extrapolated value [3]. Because of the high magnetic field and Hall parameter it is opportune to examine the effect of these parameters on voltage drops with current density treated as an independent variable. Through the use of the external battery power supplies we expect to make measurements at average current densities up to 2 amps/cm^2.

The relatively fine segmentation of the electrodes will permit shorting of the segments in twos and threes to measure current distribution as a function of β and j. Computer calculations for an electrode temperature of 2000 K and a core temperature of 2700 K at B = 6 tesla and for the expected flow conditions show a 10% - 20% - 70% distribution of current for the triplet electrode case. Experimental measurements are important because local current densities have very important effects on the operation and life times of electrodes.

The high shear stress on the insulating wall predicted by Rankin [4] may be observable at 6 tesla in the proposed experiments. The difference in pressure drop computed for a conventional boundary layer and for the modified Hartmann flow case is about 1 psi for the flow conditions of the test. This will give valuable insight when coupled with pressure drop measurements at B = 0.

Data will be observed from currents, sidewall voltage pins, and pressure transducers to investigate fluctuations at high magnetic field. The possibility of inducing transients into the system by impulsive loading of some electrode circuits with and without enhancement is being studied.

4.0 REFERENCES

[1] Kowalik, Ralph, M. and Kruger, C. H., J. Quant. Spectrosc. Radiat. Transfer, 18: 627-636 (1977).

[2] DOE Annual Report for the period July to September, 1978, Contract No. EX 76-C-01-2341, Report No. FE 2341-10, October, 1978, pp. 16-25.

[3] Kessler, R., and Eustis, R. H., "Effects of Electrode and Boundary-Layer Temperatures on MHD-Generator Performance," AIAA Journal 6, September 1968, p. 1640.

[4] Rankin, Roy, R., "Insulating Wall Boundary Layer in a Faraday MHD Generator," Ph.D. Dissertation, Stanford University, March, 1978.

*U.S. GOVERNMENT PRINTING OFFICE : 1979 0-620-097/2316